Original Research Article

Dietary *Eucommia ulmoides* leaf extract improves laying performance by altering serum metabolic profiles and gut bacteria in aged laying hens

Xiaoxiao Liang [a, 1], Yawei Fu [a, 1], Kaimin Niu [c], Zhenya Zhai [c], Hongxun Shi [d], Ruxia Wang [a, c, d, *], Yulong Yin [a, b, *]

[a] College of Animal Science and Technology, Henan Agricultural University, Zhengzhou 450002, China
[b] Institute of Subtropical Agriculture, Chinese Academy of Sciences, Changsha 410125, China
[c] Institute of Biological Resources, Jiangxi Academy of Sciences, Nanchang 330096, China
[d] Henan Ground Biological Science & Technology Co., Ltd, Zhengzhou 450001, China

ABSTRACT

The leaves of *Eucommia ulmoides* are rich in bioactive constituents that have potential gastrointestinal benefits for animals. In aged laying hens, intestinal health issues contribute to a significant decline in egg-laying capacity during intermediate and later stages. It remains unclear whether *E. ulmoides* leaf extract (ELE) can improve intestinal health and enhance egg production in elderly laying hens, and the underlying mechanisms are yet to be elucidated. Therefore, we conducted a study with 480 laying hens (65 weeks old) randomly allocated into four groups: a control group fed with the basal diet, and three treatment groups supplemented with 500, 1,000, and 2,000 mg/kg of ELE, respectively. The primary active constituents of ELE include flavonoids, polysaccharides, terpenoids, and phenolic acids. Dietary supplementation with ELE at 1,000 mg/kg (ELE1000) significantly improved laying performance and egg quality compared to the other groups. ELE1000 stimulated the maturation of intestinal epithelial cells, increased villus height, and reduced crypt depth. It also influenced the levels of proteins associated with tight junctions (claudin-1 and claudin-2) and intestinal inflammatory factors (IL-6, IL-1β, and IL-2) in different intestinal sections. Integrative analysis of serum metabolomics and gut microbiota revealed that ELE1000 improved nutrient metabolism by modulating amino acid and ubiquinone biosynthesis and influenced the abundance of intestinal microbiota by enriching pivotal genera such as *Bacteroides* and *Rikenellaceae_RC9_gut_group*. We identified 15 metabolites significantly correlated with both gut microbiota and laying performance, e.g., DL-methionine sulfoxide, THJ2201 N-valerate metabolite, tetracarbonic acid, etc. In conclusion, ELE1000 improved laying performance in elderly laying hens by affecting intestinal morphology, barrier function, microbiota, and serum metabolite profiles. These findings suggest that ELE can be a beneficial feed additive for extending the peak producing period in aged laying hens.

© 2023 The Authors. Publishing services by Elsevier B.V. on behalf of KeAi Communications Co. Ltd. This is an open access article under the CC BY-NC-ND license (http://creativecommons.org/licenses/by-nc-nd/4.0/).

1. Introduction

As the laying cycle progresses, the performance and quality of eggs from laying hens progressively diminish during the later phases of production. One noteworthy determinant is the compromised intestinal well-being of aging hens, which curtails their capacity to efficiently assimilate and metabolize nutrients. Consequently, the functionality of the digestive and absorptive processes within the intestinal tract declines, facilitating the entry of deleterious agents such as pathogens and toxins into the systemic circulation (Jing et al., 2014; Li et al., 2022a). Moreover, an

accumulating body of evidence suggests that the gut microbiota exerts a pivotal influence on modulating a diverse array of metabolic pathways in animals (Wikoff et al., 2009; Dodd et al., 2017). Consequently, the pursuit of improving intestinal health and microflora has emerged as a widely adopted and effective strategy for enhancing laying performance in domestic poultry. Historically, in-feed antibiotics were considered the primary approach for enhancing the physical well-being and productivity of agricultural animals. However, following China's ban on in-feed antibiotics in 2020, a diverse range of feed supplements, such as plant extracts (Dilawar et al., 2021), organic acids (Zhang et al., 2022a), and probiotics (Khan et al., 2020), have gained considerable popularity. Among these alternatives, botanical extracts are regarded as a reliable and efficacious choice within the realm of animal husbandry.

Eucommia ulmoides is a traditional Chinese herbal medicine that is conventionally administered topically. The residual foliage of *E. ulmoides* harbors a substantial quantity of biologically active constituents and exhibits the potential to serve as an efficacious feed supplement owing to its growth-promoting properties, antioxidant activity, and immunomodulatory effects (Dai et al., 2013; Shi et al., 2019; Xing et al., 2019). Numerous research investigations have established that *E. ulmoides* leave extract (ELE) facilitates the proliferation and productivity of various organisms, including carp (Sun et al., 2019), swine (Peng et al., 2019), and poultry (Zhao et al., 2019), and others. The extract obtained from ELE has been found to upregulate the mRNA expression levels of Takeda G-protein coupled receptor 5 (*TGR5*), claudin-1, and occludin in the colon, thereby augmenting intestinal barrier function. Furthermore, ELE has been demonstrated to enhance gut microbiota richness and diversity, while reducing the abundance of Bacteroidaceae and increasing the abundance of Akkermansiaceae and Ruminococcaceae in mice afflicted with inflammatory bowel disease (Zhai et al., 2021). The inclusion of a diet enriched with a high concentration of ELE has been shown to improve the laying rate and induce favorable alterations in the intestinal microbiota of laying hens (Peng et al., 2022). However, the precise mechanism underlying the growth-promoting effects of ELE remains elusive.

The present study aims to investigate the effects of dietary supplementation of ELE on the laying performance, intestinal health, microbiome, and serum metabolomics of elderly laying hens. It is expected that the outcomes of this investigation will provide a theoretical and practical basis for the utilization of ELE as a novel functional feed additive in poultry.

2. Materials and methods

2.1. Animal ethics statement

The ethical treatment of animals and the methodologies employed in this study underwent careful scrutiny and received approval from the Animal Care and Use Committee of the College of Animal Science and Technology, Henan Agricultural University (22-0131).

2.2. Preparation of ELE

The dehydrated foliage of *E. ulmoides* was obtained from Hengxing Co., Ltd (Zhangjiajie, China) and underwent extraction through a dual soaking method in deionized water at 75 °C for 2 h. The resultant supernatant was collected, filtered, and subsequently concentrated using a vacuum evaporator. Following this, the concentrated solution was subjected to spray-drying and sieving procedures to obtain ELE. The air temperatures employed during

the spray-drying process were set at 150 °C for the inlet and 80 °C for the outlet.

2.3. Determination of active components and small molecular metabolites in ELE

The small-molecule metabolites present in ELE were detected using liquid chromatography tandem secondary mass spectrometry (LC—MS/MS). A total of 1,830 metabolites were identified within ELE and their relative quantitative values were determined based on their chromatographic peak areas. Among the identified compounds, the top 10 bioactive constituents comprised flavonoids (18.69%), amino acids and their derivatives (11.8%), organic acids and their derivatives (8.2%), organic heterocyclic compounds (7.27%), sugars and their derivatives (7.16%), terpenes (7.10%), lipids (6.89%), alkaloids and their derivatives (6.12%), phenylpropanoids (5.63%), and phenolic acids (5.03%).

2.4. Subjects, diets, and experimental protocol

A total of 480 Hy-Line Brown laying hens at the age of 65 weeks were randomly assigned to four groups. The treatment groups were fed the basal diet supplemented with ELE at 500, 1,000, and 2,000 mg/kg, respectively, while the control group (cont) was fed the basal diet alone. The basal diet was provided by Henan Ground Biological Science & Technology Co., Ltd. (Zhengzhou, China). Table 1 presents the nutritional composition and profile of the basal diet, with the main nutrient levels determined following the previous studies (Zhang, 2007). The analysis involved the use of an automated K9860 nitrogen analyzer (manufactured by Hanon, Instrument Qingdao China) and an amino acid analyzer LA8080 (Hitachi, Japan). The feeding experiment lasted for 9 weeks, consisting of 1 week of acclimation and 8 weeks of the actual trial. Throughout the study, detailed records of egg production, egg weight, fractured eggshells, and soiled eggs were meticulously kept, and weekly feed consumption was recorded. On 56 d of the trial, the laying rate per replicate, average egg weight, daily feed intake, feed conversion ratio, percentage of broken eggs, and percentage of soiled eggs were all calculated.

Table 1
Ingredients and nutrient level of the basal diet (air-dry basis, %).

Item	Content
Ingredients	
Corn	61.0
Soybean meal	25.0
Limestone	8.0
Minerals premix[1]	1.0
Soybean oil	5.0
Total	100
Nutritional level[2]	
Metabolizable energy, MJ/kg	11.23
Crude protein	16.0
Lysine	0.82
Methionine	0.36
Calcium	3.55
Total phosphorus	0.48

[1] Premix provided the following per kilogram of the diet: vitamin A 9,500 IU, vitamin D_3 3,000 IU, vitamin E 36.5 IU, vitamin K_3 2.25 mg, thiamine 5.0 mg, riboflavin 7.0 mg, calcium pantothenate 20 mg, niacin 49 mg, pyridoxine 11 mg, biotin 0.25 mg, folic acid 1.5 mg, vitamin B_{12} 0.017 mg, choline 1,200 mg, Mn 112 mg, I 0.45 mg, Fe 140 mg, Cu 17 mg, Zn 108 mg, Se 0.4 mg.
[2] Metabolizable energy (ME) was calculated, while the others were measured. ME = Corn × ME1 + Soybean × ME2 + Limestone × ME3 + Minerals premix × ME4 + Soybean oil × ME5. All values of ME1 to ME5 were drawn from the Chinese Feed Composition and Nutritional Value Table (32th edition, 2021), Chinese feed database (Xiong, 2021).

2.5. Sample collection

At the end of the 56-d trial, the birds were weighed and subjected to a 12-h fasting period before being euthanized on 57 d of the trial at 08:00. Blood samples were collected and kept at room temperature for serum isolation through centrifugation at $2,000 \times g$ for 15 min at 4 °C. The serum was then stored at −20 °C for subsequent analysis. Tissue samples from the duodenum, jejunum, and ileum were immediately excised. A 2-cm segment from the middle portion was dissected, rinsed with sterile saline, and placed in Bouin's solution for a minimum of 48 h while being protected from light. Additional intestinal tissues were collected and preserved in liquid nitrogen for molecular examinations. The contents of the jejunum, ileum, duodenum, and cecum were extracted, transferred to containers, rapidly frozen with liquid nitrogen, and maintained at a −80 °C.

2.6. Egg quality measurement

On 56 d of the trial, eggs were collected and a random sample of 5 eggs was chosen from each cluster. The longitudinal and transverse dimensions of the eggs, as well as the thickness of the pointed, median, and rounded shells, were assessed using an electronic Vernier caliper (Deli, DL3944, Ningbo). An electronic balance (Leqi, LQ-A20002, Suzhou) was used to measure the absolute mass of both the egg yolk and its calcareous shell. The strength of the eggshell was evaluated using an eggshell toughness measuring instrument (Nanjing Mingao Instrument and Equipment Co., Ltd). Furthermore, the egg weight, yolk pigmentation, and Haugh unit were determined using an Egg Analyzer, an automatic device for assessing egg quality (Orka Technology Group Ltd). The egg morphology was characterized by evaluating the egg shape index, which represents the ratio of the longitudinal diameter to the transverse diameter. The eggshell thickness was determined by calculating the average thickness at the pointed end, equator, and blunt end. Additionally, the yolk ratio, expressed as the percentage of yolk weight relative to egg weight, was calculated.

2.7. Intestinal morphology

After the designated intestinal segment was removed, the tissue was carefully trimmed using a scalpel and then dehydrated and made transparent. Subsequently, the tissue was embedded in wax and cut into paraffin blocks. The sections were stained with hematoxylin and eosin (H&E) staining and sealed with gum. Six cross-sectional segments were obtained from each intestinal sample, and 3 to 5 representative visual fields were selected from each section. The height of the intestinal villi (VH) and the depth of the crypts (CD) were quantified using the NIS-Elements microscopic image analysis software (Nikon Instruments, Tokyo, Japan) and the VH:CD ratio was calculated.

2.8. Real-time quantitative PCR (RT-qPCR) and RNA isolation

The manufacturer's protocols and instructions (Magzol; Magen, Guangzhou, China) were followed to extract total RNA from intestinal tissue samples. The purity and yield of the RNA were evaluated using the NanoDrop 1000 equipment (Thermo Fisher Scientific, New York, NK, USA). Subsequently, reverse transcription of messenger RNA was performed using Prime Script RT reagent Kits (Takara, Tokyo, Japan). The primers used in this study were designed using the Primer 5.0 software package, and their respective sequences are presented in Table 2. The gene expression levels were analyzed using SYBR green-based quantitative real-

Table 2
RT-PCR specific primer sequences.

Genes	Accession number	Primer 5′–3′	Product size, bp
Occludin	NM_205128.1	F:GCAGATGTCCAGCGGTTACTAC R:CGAAGAAGCAGATGAGGCAGAG	176
ZO-2	NM_001396728.1	F:TCACCTTCTTCTTCTTCCCAATCT R:GCAACCTTCCGTCCATCTC	89
ZO-1	XM_021098896.1	F:CCAACCATGTCTTGAAGCAGC R:TGCAGGAGTGTGGTCTTCAC	215
Claudin-1	NM_001244539.1	F:AAGGACAAAACCGTGTGGGA R:CTCTCCCCACATTCGAGATGATT	247
Claudin-2	NM_001277622.1	F:CTCAGCCCTCCATCAAACA R:TGCTGCTGCTACACGTAT	82
TLR-4	NM_001030693.2	F:GTTCCTGCTGAAATCCCAAA R:TATGGTAGTGGCACCTTGAA	133
IFN-γ	NM_205149.2	F:ACAGGCAAACAATGGAAGT R:CAGGTCAACAAACATACAACA G	96
TNF-α	NM_001396917.1	F:CAGAGCTCCTTTTGCTCCGT R:GCTCTGTGAAACTTAACTCCTCCT	129
IL-1β	NM_204524.2	F:TTCATTACCGTCCCGTTG R:GCTTTTATTTCTCCAGTCACA	121
IL-6	NM_204628.2	F:GGTGATAAATCCCGATGAAGT R:CTCCATAAACGAAGTAAAGTCTC	139
IL-2	NM_201453.2	F:AACCTGCTGTCCA R:GCCCGTAGGGCTTACAGAAA	99
β-Actin	NM_205518	F:TGCGTGACATCAAGGAGAAG R:TGCCAGGGTACATTGTGGTA	300
GAPDH	NM_204305.2	F:CTACACACGGACACTTCAAG R:ACAAACATGGGGGCATCAG	244

ZO-1 = zonula occludens 1; ZO-2 = zonula occludens 2; TLR-4 = toll-like receptor 4; IFN-γ = interferon gamma; TNF-α = tumor necrosis factor-alpha; IL-1β = interleukin 1 beta; IL-6 = interleukin 6; IL-2 = interleukin 2; GAPDH = glyceraldehyde-3-phosphate dehydrogenase.

time PCR with the ABI Prism 7900 HT Sequence Detection System (Applied Biosystems, Foster, CA, USA). The β-actin gene was used as an internal reference to standardize the target gene levels, and the relative mRNA expression of the target genes was calculated as a ratio to the mRNA level of the β-actin gene using the $2^{-\triangle\triangle Ct}$ technique.

2.9. Sequencing and analysis of the 16S rRNA gene amplicons

The genomic DNA from the cecum digesta was extracted using the CTAB method. The V4 region of the 16S rRNA gene was amplified using specific primers, namely 515F (ACTCCTACGG-GAGGCAGCAG) and 806R (GGACTACHVGGGTWTCTAAT). Subsequently, the PCR product mixture underwent purification with the Qiagen Gel Extraction Kit (Qiagen, Germany), followed by quantification using a Qubit 2.0 Fluorometer (Thermo Scientific) and the Agilent Bioanalyzer 2100 system (Agilent Technologies, Palo Alto, CA). The purified product was then subjected to sequencing using an Illumina NovaSeq 2500 platform (Illumina, USA). The raw sequencing data was processed using the QIIME software suite. The Uparse program was utilized to cluster operational taxonomic units (OTU) based on a similarity threshold of less than 97%. Further annotation was performed on the representative sequence of each OTU. Alpha and beta diversity metrics, including weighted and unweighted UniFrac, were calculated using the QIIME software (Version 1.9.1). Alpha diversity was assessed using observed-species, Chao1, Shannon, Simpson, and the ACE index. Beta diversity was analyzed using multivariate statistical methods to compare differences between the two groups. The obtained data was then subjected to predictive functional inference for microbial communities (PICRUSt), which identified distinct metabolic pathways and functions between the two groups. The PICRUSt bioinformatics software tool was utilized to predict KEGG database-compliant functions based on the 16S sequencing data.

Additionally, Spearman analysis was conducted to evaluate the correlation between differentially abundant bacterial genera and serum metabolites.

2.10. Determination and analysis of serum metabolites

Non-targeted metabolomics and LC-MS/MS technology were employed by Novogene Biotech Co. (Beijing, China) to investigate the serum metabolites. Serum sample preparation and LC-MS/MS analysis were conducted following a previously established protocol (Sun et al., 2019). Metabolites were deemed differentially expressed if they exhibited a VIP score greater than 1, a P-value less than 0.05, and a fold change (FC) greater than 2 or less than 0.5. The identified metabolites underwent functional annotation using the KEGG database, and the annotated metabolites were mapped onto the KEGG pathway database. A metabolic pathway enrichment analysis was conducted based on the criterion of $x/n > y/N$, and pathways meeting this criterion were considered enriched. Furthermore, metabolic pathways with a P-value less than 0.05, indicative of statistical significance, were identified in terms of their enrichment.

2.11. Statistical analysis

The statistical analysis was performed using SPSS software (version 22.0, SPSS Inc., Chicago, IL). The data were presented as means and SEM, and group comparisons were conducted using T-tests and One-way ANOVA. Statistical significance was considered at a P-value threshold less than or equal to 0.05, while P-values ranging from 0.05 to 0.10 were regarded as indicative of trends.

3. Results

3.1. Effect of ELE supplementation on the performance of laying

Table 3 presents the impacts of dietary supplementation of ELE on the productivity of aged laying hens in egg production. The die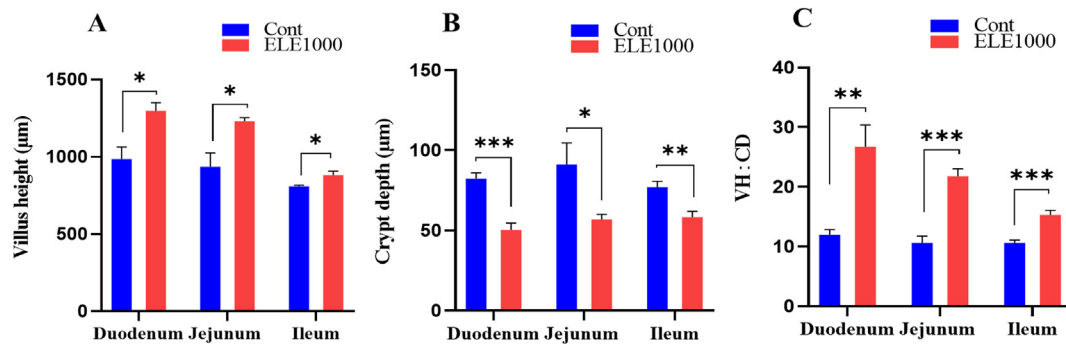tary supplementation of ELE at 1,000 mg/kg (ELE1000) treatment group exhibited significantly higher egg-laying rates compared to the other groups ($P = 0.13$), accompanied by decreased feed conversion ratios ($P = 0.10$) and rates of soiled eggs ($P = 0.00$). Nevertheless, there were no significant effects observed on the occurrences of cracked eggs, average egg weight, or daily feed consumption ($P > 0.05$). In summary, ELE1000 resulted in an enhanced egg-laying performance.

### 3.2. Effect of ELE supplementation on egg quality

Table 4 presents the influence of ELE supplementation on the quality of eggs. The ELE1000 treatment group exhibited significant improvements in egg weight ($P = 0.03$), eggshell strength ($P = 0.01$), and yolk color ($P = 0.00$) compared to the other groups. Interestingly, as the dosage of ELE supplementation increased in the ELE2000 group, there was a notable decrease in the Haugh unit compared to the other groups ($P = 0.01$). Overall, the supplementation of ELE in the diet resulted in enhanced egg quality. Notably, the ELE1000 group demonstrated superior performance and egg quality compared to the other groups. Consequently, the ELE1000 group was selected for further analyses.

3.3. Effect of ELE1000 supplementation on intestinal morphology, integrity, and immunity

The impact of dietary inclusion of 1,000 mg/kg ELE on intestinal morphology, integrity, and immunity is depicted in Figs. 1 and 2. In comparison to the control group, the ELE1000 group exhibited significant improvements in villus height (Fig. 1A, $P < 0.05$), the ratio of villus height to crypt depth (Fig. 1C, $P < 0.05$), and reduced crypt depth (Fig. 1B, $P < 0.05$) in the jejunum, ileum, and duodenum. Furthermore, the addition of 1,000 mg/kg ELE resulted in an increase in claudin-1 mRNA expression in the duodenum (Fig. 2A1, $P = 0.05$) and ileum (Fig. 2C1, $P = 0.08$), while decreasing claudin-2 mRNA expression in the jejunum (Fig. 2B1, $P = 0.01$), indicating a propensity for improved intestinal integrity. These findings suggest that the dietary inclusion of ELE may enhance the intestinal structure of laying hens and influence gut integrity. Furthermore, the

Table 3
Effect of *E. ulmoides* leaf extract (ELE) on performance of aged laying hens.

Item	Supplementary level of ELE, mg/kg				SEM	P-value		
	0	500	1,000	2,000		Intergroup	Linear	Quadratic
Daily feed intake, g	120.75	118.15	119.63	120.94	1.21	0.86	0.86	0.45
Laying rate, %	76.54	80.26	84.33	79.61	1.17	0.13	0.19	0.07
Average egg weight, g	67.88	65.83	65.74	65.94	1.26	0.93	0.63	0.68
Feed conversion ratio	2.37	2.25	2.18	2.32	0.03	0.10	0.36	0.02
Egg-broken rate, %	1.10	0.86	0.62	1.17	0.11	0.31	0.95	0.09
Dirty eggs rate, %	4.67[a]	1.80[b]	1.81[b]	2.64[b]	0.29	0.00	0.00	0.00

Values within a row that do not share a common superscript are significantly different ($P < 0.05$).

Table 4
Effect of *E. ulmoides* leaf extract (ELE) on egg quality of aged laying hens.

Item	Supplementary level of ELE, mg/kg				SEM	P-value		
	0	500	1,000	2,000		Intergroup	Linear	Quadratic
Egg weight, g	61.92[b]	64.61[a]	64.35[a]	63.76[ab]	0.37	0.03	0.08	0.02
Egg shape index	1.31	1.31	1.32	1.31	0.003	0.77	0.75	0.81
Eggshell strength, N	24.97[b]	24.82[b]	30.48[ab]	34.40[a]	1.32	0.01	0.00	0.36
Eggshell thickness, mm	0.26	0.25	0.27	0.26	0.01	0.63	0.65	0.95
Eggshell weight, g	5.15	5.44	5.28	5.28	0.07	0.58	0.74	0.33
Egg yolk color	6.33[b]	7.45[a]	7.61[a]	6.95[a]	0.16	0.00	0.02	0.00
Yolk rate, %	29.23	29.41	29.31	28.06	0.45	0.70	0.39	0.44
Haugh unit	57.38[a]	59.00[a]	59.18[a]	44.75[b]	1.93	0.01	0.01	0.02

Values within a row that do not share a common superscript are significantly different ($P < 0.05$).

Fig. 1. Effects of dietary *E. ulmoides* leaf extract (ELE) supplementation on the intestinal morphology of aged laying hens. (A) The villus height, (B) crypt depth, and (C) villus height-to-crypt depth (VH:CD) ratio in the duodenum, jejunum and ileum. Data are expressed as means ± SEM (n = 6). Asterisks indicate significant differences as per the T-test (*P < 0.05, **P < 0.01, ***P < 0.001). VH = villus height; CD = crypt depth; Cont = basal diet; ELE1000 = basal diet + 1,000 mg/kg of ELE.
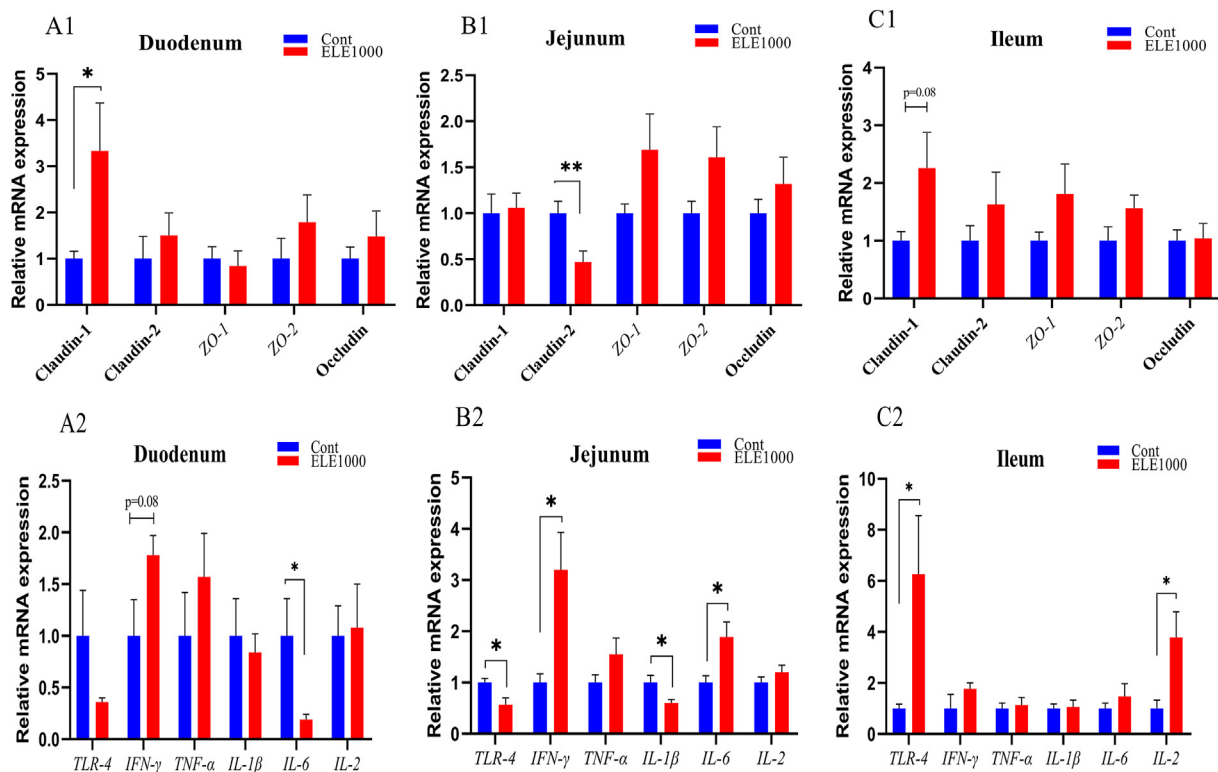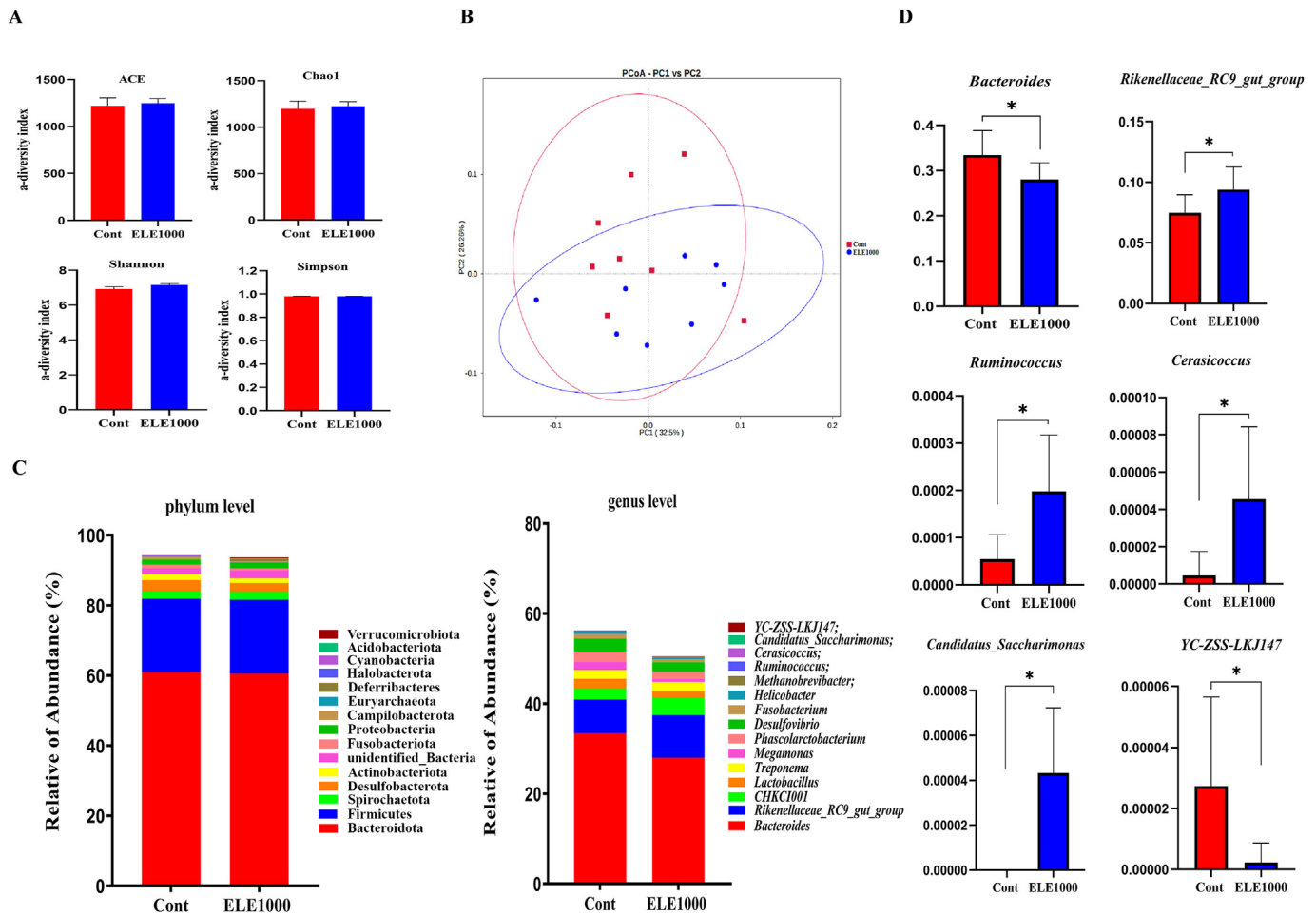

Fig. 2. Effects of *E. ulmoides* leaf extract (ELE) on the expression of intestinal tight junction protein and intestinal-related cellular immune factor mRNA in aged laying hens. The mRNA expression of tight junction protein in duodenum (A1), jejunum (B1) and ileum (C1). The mRNA expression of intestinal-related cellular immune factor in duodenum (A2), jejunum (B2) and ileum (C2). Data are expressed as means ± SEM (n = 6). Asterisks indicate significant differences as per the T-test (*P < 0.05, **P < 0.01). Cont = basal diet; ELE1000 = basal diet + 1,000 mg/kg of ELE; *ZO* = zonula occludens; *TLR-4* = toll-like receptor 4, *IFN*-γ = interferon γ, *TNF*-α = tumor necrosis factor-alpha, *IL* = interleukin.

mRNA expression of immune-related components was further investigated. Compared to the control group, the addition of 1,000 mg/kg ELE significantly reduced the mRNA expression of interleukin (*IL*)-6 (P = 0.05) (Fig. 2A2) and demonstrated a tendency to up-regulate the expression of interferon (*IFN*)-γ (P = 0.08) (Fig. 2A2) in the duodenum. In the jejunum, the ELE1000 group exhibited higher mRNA expressions of *IL*-6 (P = 0.02) and *IFN*-γ (P = 0.02) and lower mRNA expressions of Toll-like receptor (*TLR-4*) (P = 0.02) and *IL-1β* (P = 0.03) compared to the control group (Fig. 2B2). Additionally, the dietary inclusion of 1,000 mg/kg ELE significantly increased the mRNA expression of *TLR-4* (P = 0.05) and *IL-2* (P = 0.02) in the ileum (Fig. 2C2). These findings suggest that ELE modulates the intestinal immune response by promoting the secretion of immune factors within the intestines.

3.4. Effects of ELE1000 supplementation on the gut microbiome of laying hens

Fig. 3 presents additional analysis regarding the effects of 1,000 mg/kg ELE supplementation on gut bacterial diversity and composition. In comparison to the control group, the addition of ELE at a dose of 1,000 mg/kg did not significantly influence the microbiota's α-diversity, as indicated by the ACE, Chao1, Simpson, and Shannon indices (Fig. 3A, P > 0.05). The PCoA analysis revealed significant similarities between the gut microbiota of the ELE1000 group and the control group (Fig. 3B, P > 0.05). Furthermore, no notable differences were observed between the two groups in terms of the core microbiota at the phylum and genus levels (Fig. 3C, P > 0.05). However, it was observed that the inclusion of

Fig. 3. Effects of *E. ulmoides* leaf extract (ELE) supplementation on gut microbiota composition of aged laying hens. (A) Alpha-diversity: Chao 1, ACE, Shannon and Simpson. (B) Beta-diversity of gut microbiota. (C) Relative abundance of gut microbiota at the phylum level and genus level. (D) Differential bacterial genus relative abundance at the genus level. Data are expressed as means ± SEM ($n = 8$). Asterisks indicate significant differences as per the T-test (*$P < 0.05$). Cont = basal diet; ELE1000 = basal diet + 1,000 mg/kg of ELE; PCoA = principal coordinates analysis.

ELE1000 significantly increased the relative abundance of *Candidatus_Saccharimonas*, *Ruminococcus*, *Cerasicoccus*, and *Rikenellaceae_RC9_gut group* at the genus level, while decreasing the relative abundance of *Bacteroides* and *YC-ZSS-LKJ147* (Fig. 3D, $P < 0.05$).
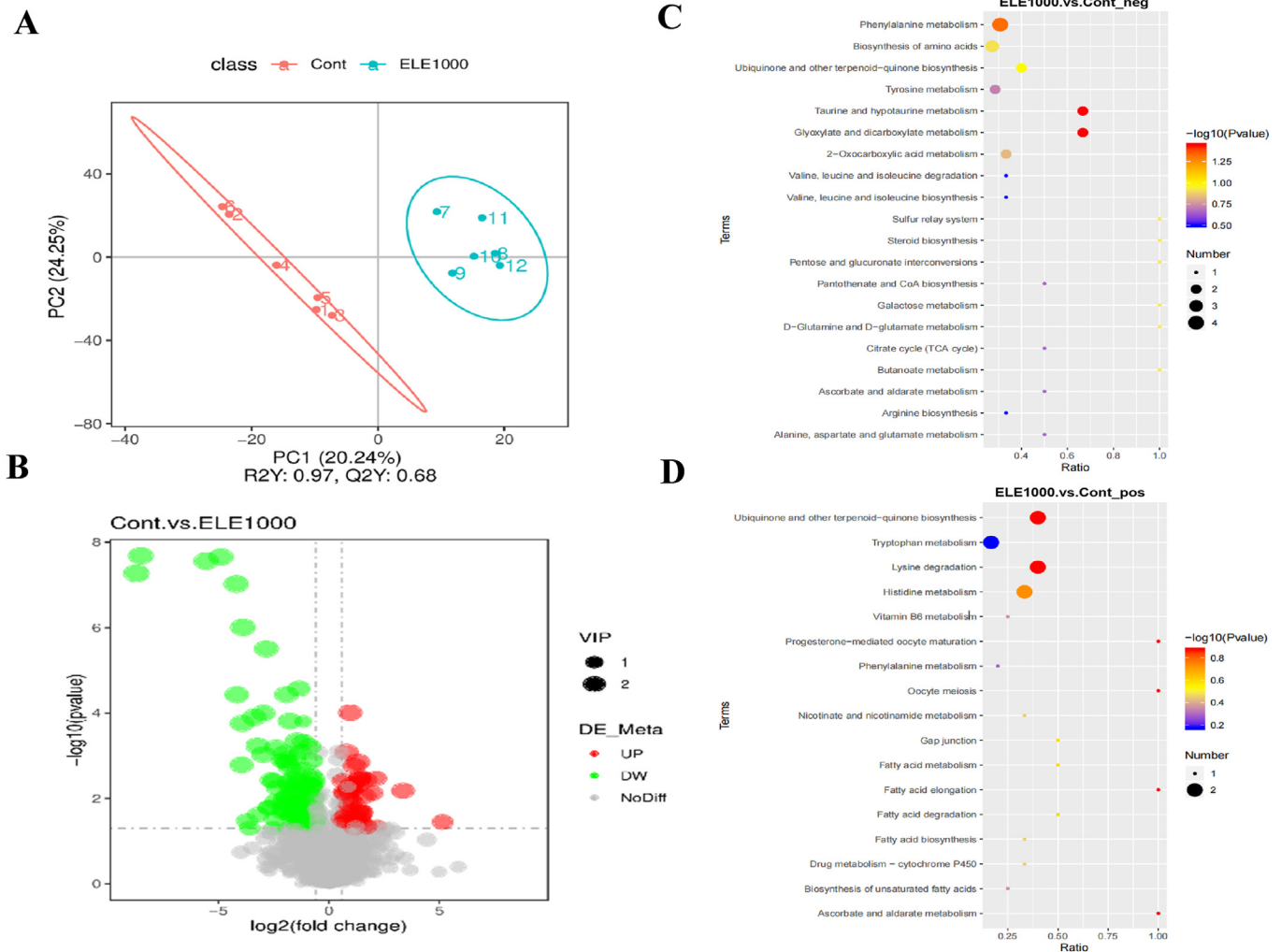
3.5. Effects of ELE1000 supplementation on serum metabolites

Further analysis was conducted to examine the impact of feed supplementation of 1,000 mg/kg ELE on changes in blood metabolites. The results demonstrated distinct clustering of the two groups in the partial least squares discrimination analysis (PLS-DA) (Fig. 4A), indicating that ELE1000 supplementation significantly altered the serum metabolite profile. The heat map illustrating the clustered differential metabolites between the control and ELE groups revealed noticeable metabolic differences. Moreover, the overall distribution of differential metabolites is depicted in the volcano plot of Fig. 4B. A total of 125 metabolites exhibited significant alterations, including 90 up-regulated and 35 down-regulated metabolites, in both positive and negative screening models. From these changed metabolites, 40 metabolites were further selected based on specific criteria such as VIP > 1, *P*-value < 0.05, and FC > 2 or FC < 0.5, as depicted in Fig. 5A and B.

KEGG pathway analysis was conducted to investigate the impact of dietary ELE supplementation on the metabolic pathways of laying hens. The metabolites affected by ELE were found to be primarily involved in 21 metabolic pathways, as depicted in Fig. 4C and D. The positive ion mode pathways included ubiquinone and other terpenoid-quinone biosynthesis, tryptophan metabolism, histidine metabolism, progesterone-mediated oocyte maturation, oocyte meiosis, fatty acid elongation, and ascorbate and aldarate metabolism. Conversely, the negative ion mode pathways encompassed phenylalanine metabolism, biosynthesis of amino acids, tyrosine metabolism, taurine and hypotaurine metabolism, glyoxylate and dicarboxylate metabolism, 2-oxocarboxylic acid metabolism, sulfur relay system, steroid biosynthesis, pentose and glucuronate interconversions, galactose metabolism, and D-glutamine and D-glutamate metabolism, as well as butanoate metabolism.

3.6. The correlation between the primary differential serum metabolites and differential gut bacteria

Fig. 6 illustrates the correlation between the primary differential serum metabolites and intestinal microbiota. A significant negative association was observed between serum differential metabolites and differential bacteria. Furthermore, up-regulated differential
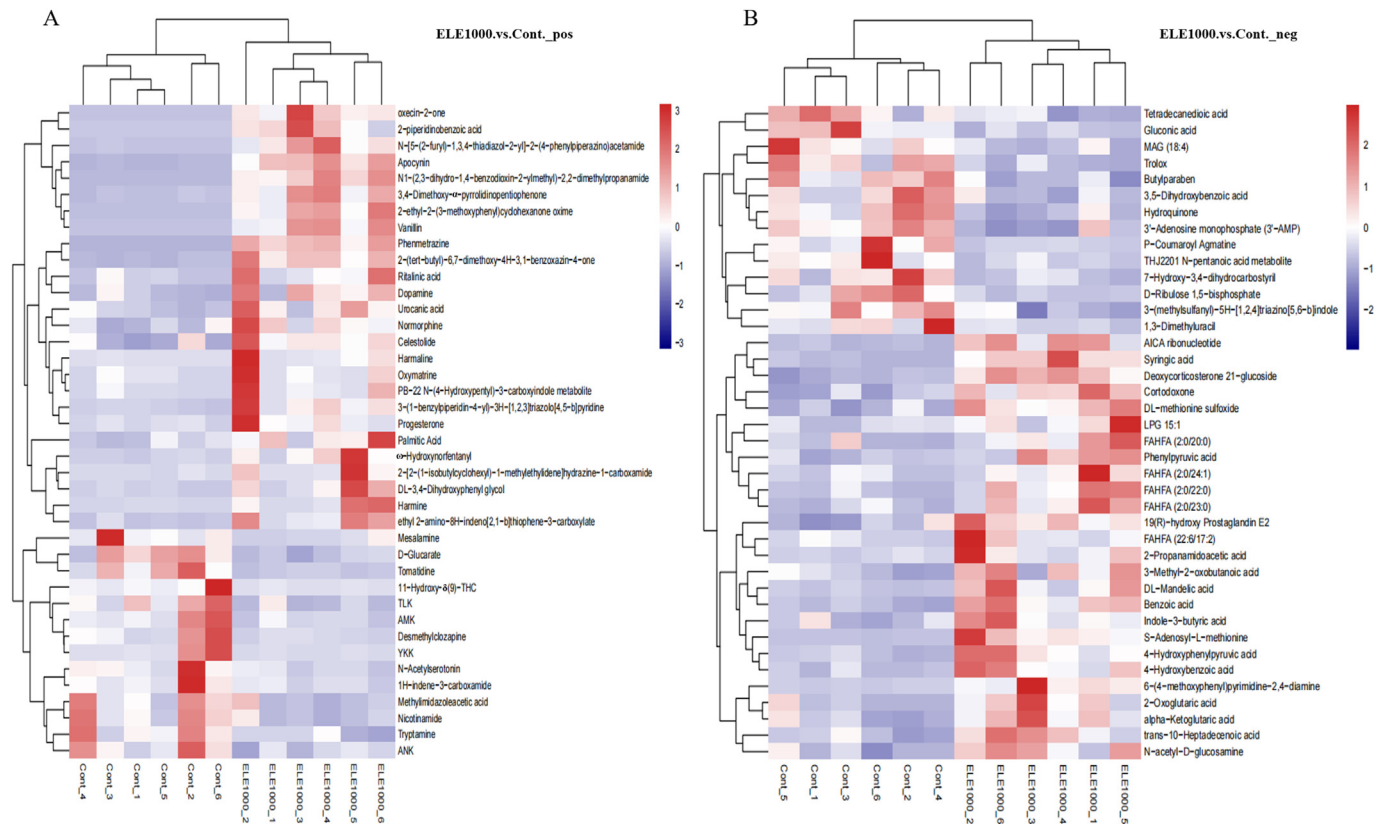
Fig. 4. Effects of *E. ulmoides* leaf extract (ELE) supplementation on serum metabolic profiles of aged laying hens (*n* = 6). (A) Orthogonal partial least squares-discriminant analysis (OPLS-DA) scores plot for the Control and ELE1000 groups for serum metabolites. (B) Volcanic diagram. Each point represents a metabolite. The significantly up-regulated metabolites are represented by red dots, while down-regulated metabolites are represented by green dots. (C and D) Serum differential metabolites enriched in the negative ion mode and positive ion mode by Kyoto Encyclopedia of Genes and Genomes (KEGG). The color of the spot indicates *P*-value. The redder, the more significant enrichment. The size of the spot represented the number of different metabolites enriched. Cont = basal diet; ELE1000 = basal diet + 1,000 mg/kg of ELE.

metabolites exhibited a positive correlation with differential bacteria, while down-regulated differential metabolites showed a negative correlation with them, and vice versa. Utilizing a correlation coefficient and *P*-value threshold (CC > 0.7 and *P* < 0.05), we identified 30 robustly phased differential metabolites with significant differences among them. Among these are in the negative ion mode including phenylpyruvic acid, 2-oxoglutaric acid, alpha-ketoglutaric acid, S-adenosyl-L-methionine, 19(R)-hydroxyprostaglandin E2, AICA ribonucleotide, 4-hydroxybenzoic acid, benzoic acid, FAHFA (2:0/22:0), LPG15:1, FAHFA (2:0/23:0), DL-methionine sulfoxide, cortodoxone, 3-methyl-2-oxobutanoic acid, THJ2201 N-pentanoic acid metabolite, Trolox, tetradecanedioic acid, and gluconic acid. Additionally, 12 metabolites were detected in the positive ion mode, namely, 2-piperidinobenzoic acid, 2-(tert-butyl)-6,7-dimethoxy-4H-3,1-benzoxazin-4-one, 3,4-dimethoxy-α-pyrrolidinopentiophenone, 3-(1-benzylpiperidin-4-yl)-3H-[1,2,3]triazolo[4,5-b]pyridine, ethyl 2-amino-8H-indeno[2,1-B]thiophene-3-carboxylate, palmitic acid, harmine, ritalinic acid, DL-3,4-dihydroxyphenyl glycol, urocanic acid, D-glucarate, and tomatidine. These findings provide evidence of a close relationship between differential bacteria and serum differential metabolites induced by ELE.

3.7. Analysis of the relationship between laying performance of laying hens and serum differential metabolites

Fig. 7 illustrates the correlation between serum differential metabolites in laying hens and their laying performance. There were 28 differential metabolites that exhibited a strong correlation with production performance (CC > 0.75 and *P* < 0.05). Among them, 18 differential metabolites were detected in the negative ion mode, including syringic acid, trans-10-heptadecenoic acid, 2-oxoglutaric acid, alpha-ketoglutaric acid, AICA ribonucleotide, FAHFA (2:0/22:0), 4-hydroxyphenylpyruvic acid, benzoic acid, cortodoxone, DL-mandelic acid, S-adenosyl-L-methionine, 4-Hydroxybenzoic acid, DL-methionine sulfoxide, FAHFA (2:0/20:0), butylparaben, 1,3-dimethyluracil, tetradecanedioic acid, and THJ2201 N-pentanoic acid metabolite. The remaining 10 differential metabolites were detected in the positive ion mode, including 2-piperidinobenzoic acid, ethyl 2-amino-8H-indeno(2,1-b)thiophene-3-carboxylate, tryptamine, phenmetrazine, YKK, tomatidine, 3-(1-benzylpiperidin-4-yl)-3H-[1,2,3]triazolo[4,5-b]pyridine, n-[5-(2-furyl)-1,3,4-thiadiazol-2-yl]-2-(4-phenylpiperazino)acetamide, 2-ethyl-2-(3-methoxyphenyl)cyclohexanone oxime, and

Fig. 5. Effects of *E. ulmoides* leaf extract (ELE) supplementation on serum metabolic profiles of aged laying hens (*n* = 6). (A) The heat map and hierarchical clustering of ELE-induced differential metabolites in the positive ion mode (A) and negative ion mode (B).

2-[2-(1-isobutylcyclohexyl)-1-methylethylidene]hydrazine-1-carboxamide (Fig. 7).

3.8. Screening of differential serum metabolites associated with distinctive bacterial strains and laying performance

As illustrated in Fig. 8, a total of 15 metabolites displayed a strong correlation with differential bacteria and laying efficiency in laying hens, such as S-adenosyl-L-methionine, benzoic acid, DL-methionine sulfoxide, THJ2201 N-valerate metabolite, tetracarbonic acid, etc., as determined through correlation analysis of serum metabolites with varying bacteria and performance. Furthermore, as depicted in Fig. 9, the relative levels of these 15 differential metabolites exhibited changes in the ELE1000 group compared to the control group. Notably, 12 of these serum differential metabolites were significantly higher in the ELE1000 group than in the control group, while 3 serum differential metabolites showed significant reduction in the control group.

4. Discussion

In comparison to the other dosage groups in the present study, the inclusion of ELE at 1,000 mg/kg demonstrated superior enhancements in laying performance and egg quality. This is in line with the findings of Zhao et al. (2019), who revealed that supplementation with chlorogenic acid-enriched extract at 1,000 mg/kg improved the growth performance of heat-stressed broilers, whereas a dosage of 500 mg/kg did not have a

noticeable effect. These results suggest the existence of an optimal dosage range for ELE supplementation in laying hens. Other studies have also reported that providing hens with ELE at the appropriate dosage can enhance their laying efficiency and reduce their feed conversion ratio (Peng et al., 2022; Yan et al., 2022).

The intestinal tract plays a pivotal role in the assimilation of nutrients and the functioning of the immune system. Intestinal morphology serves as a crucial metric for evaluating optimal intestinal performance. Traditionally, longer villi, shorter crypts, and a reduced VH:CD ratio indicate a more favorable intestinal condition (Ding et al., 2020; Zhang et al., 2022b). A prior investigation unveiled that the inclusion of ELE in the diet resulted in an enhancement of jejunum morphology and immune function, thereby ultimately promoting the growth performance of weaned piglets (Peng et al., 2019). Our study has demonstrated that ELE supplementation led to an increase in villus height and VH:CD ratio, as well as a decrease in crypt depth of the jejunum and ileum. Additionally, intestinal tight junction proteins play a critical role in maintaining the stability and permeability of the intestinal epithelial barrier, which serve to safeguard the internal environment of the body from harmful elements such as infections and toxins (Capaldo et al., 2017). In the present investigation, it was observed that the addition of ELE heightened the gene expression of claudin-1 in the duodenum and ileum, while decreasing the gene expression of claudin-2 in the jejunum. Furthermore, ELE supplementation elevated the expression of IL-6 in the jejunum while reducing its expression in the duodenum. Inconsistent mRNA expression in tissues is commonplace as the expression of certain
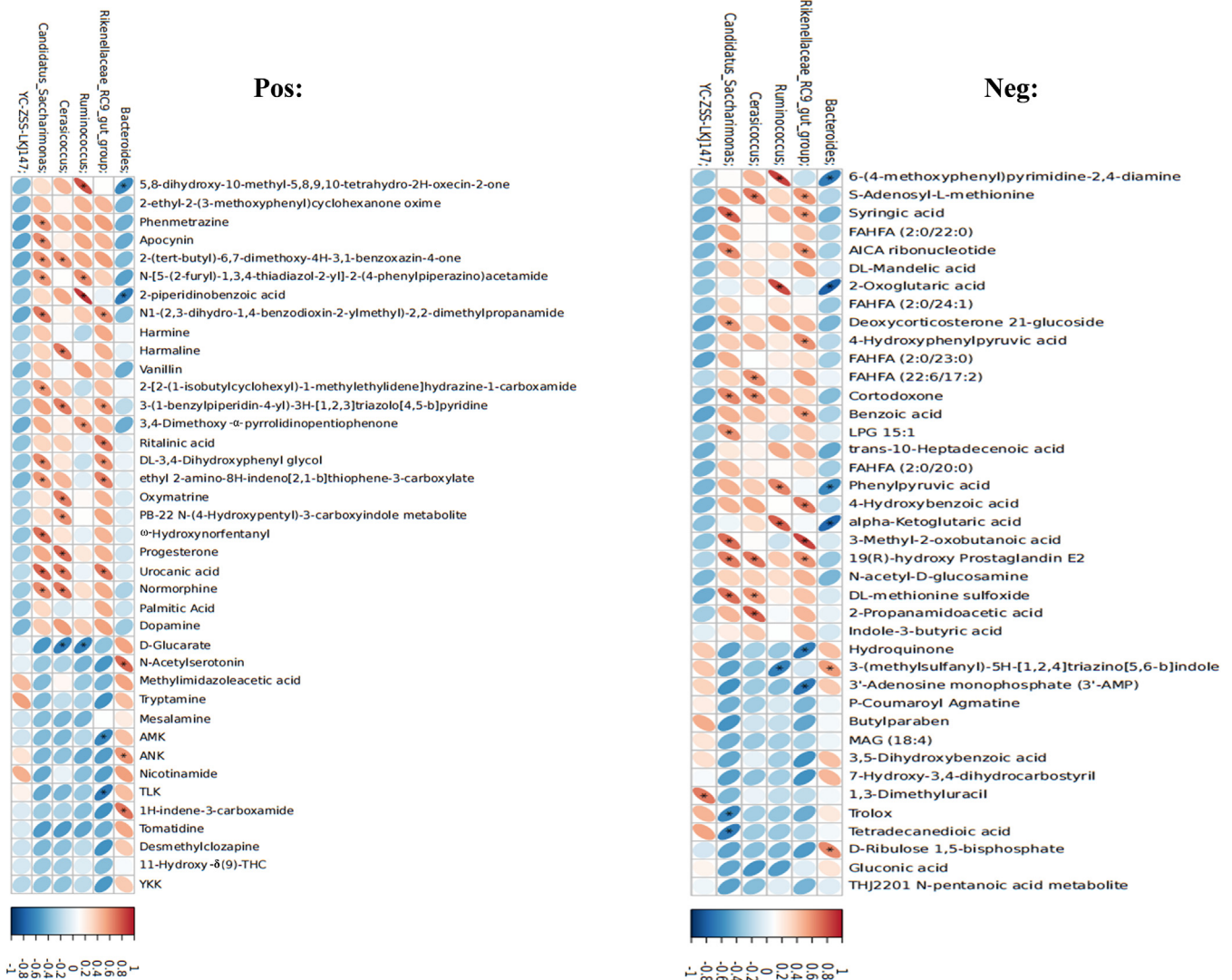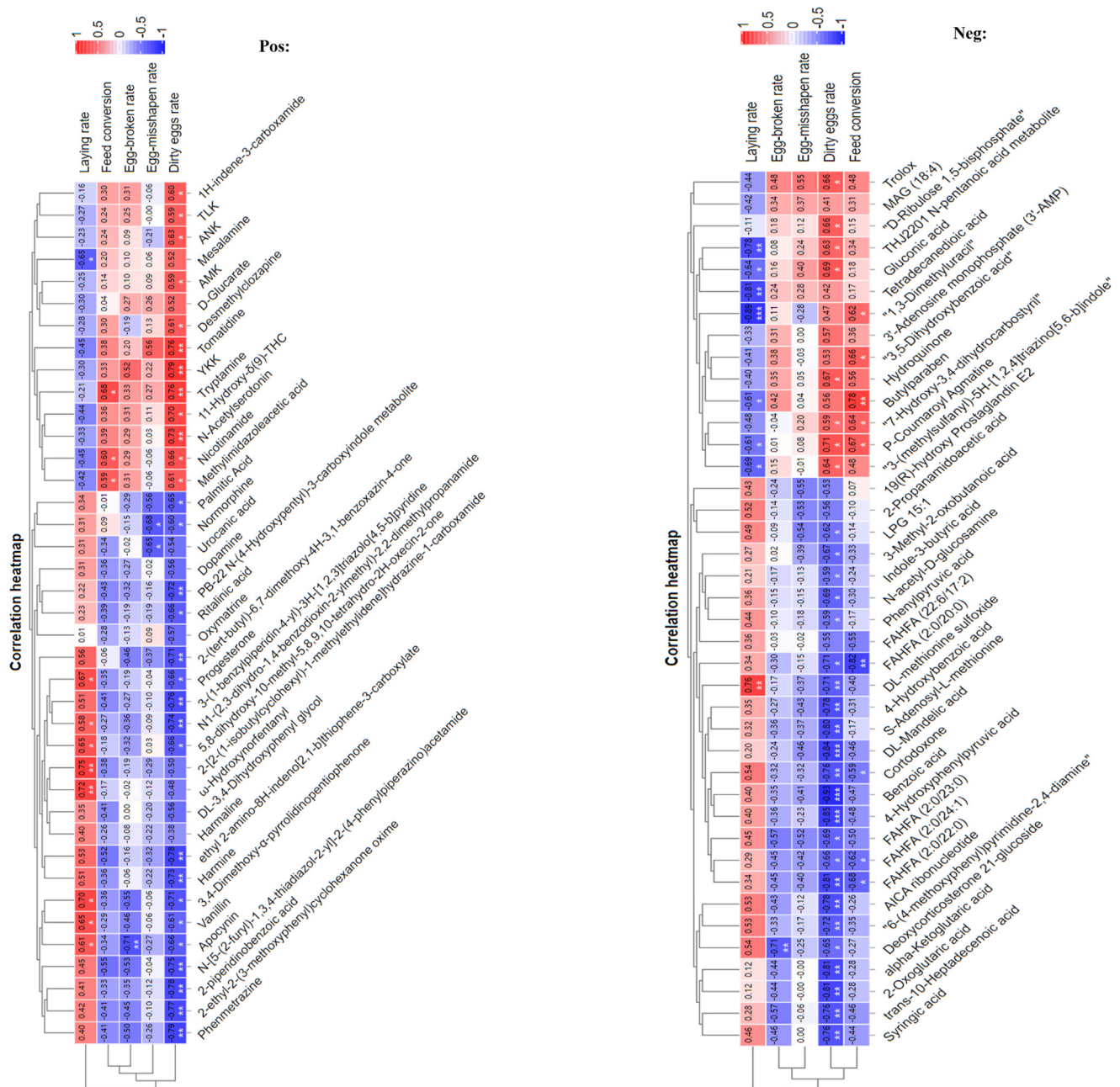
Fig. 6. Correlations between serum differential metabolites and differential bacterial genera of aged laying hens ($n = 6$). Red and blue cells represent positive and negative correlations, respectively. The significant correlations are indicated by asterisks (*$P < 0.05$).

genes fluctuates over time. Studies have reported incongruous expression of tight junction protein mRNA and protein, as well as phenotypic variability along the intestinal tract, which may be attributed to post-transcriptional regulatory mechanisms (Akbari et al., 2014). Moreover, it is evident that ELE regulates immune-related factors in the gut of hens. Similar observations have been made in pigs, where ELE has been found to enhance the expression of tight junction proteins and immune factors in the colon (Zhai et al., 2021). The aforementioned findings suggest that ELE modulates intestinal integrity by regulating structural and immune factors in aged laying hens.

An expanding body of research has established a robust correlation between alterations in the intestinal microbiota and various physiological systems, encompassing metabolism, immunity, digestion and absorption, as well as disease prevention (Hsieh and Yen, 2000; Hildebrand et al., 2013; Marchesi et al., 2016). Multiple investigations have indicated that the administration of ELE can modulate the composition of the intestinal microbiota, thereby influencing animal performance (Zhang et al., 2019; Zhao et al., 2020; Zhai et al., 2021). In accordance with prior research

(Martens et al., 2011; Sun et al., 2021), *Bacteroides*, renowned for their ability to degrade dietary fiber and glycan, exhibited significantly reduced abundance in the current study with ELE supplementation. Conversely, *Rikenellaceae_RC9_gut_group*, a species known for its capacity to ferment carbohydrates, exhibited an increase in relative abundance in response to ELE (Rowland et al., 2018). Their findings demonstrated that ELE supplementation significantly reduced the abundance of Bacteroidaceae while increasing the abundance of Akkermansiaceae and Ruminococcaceae in mice with induced inflammatory bowel disease (IBD). *Bacteroides* have been documented to contribute to the development of IBD and exacerbate the condition through enterotoxin production, mucin degradation, TLR activation, and stimulation of pro-inflammatory cytokine secretion (Rodriguez-Palacios et al., 2018; Ryan et al., 2020). Conversely, *Rikenellaceae_RC9_gut_group* belongs to the Rikenellaceae family and has demonstrated beneficial effects in both human and animal populations (Tavella et al., 2021; Lin et al., 2021). Rikenellaceae produce the short-chain fatty acids, acetate and propionate, which may serve as modulators of adiposity (Lu et al., 2016). The significance of elevated levels

Fig. 7. Correlations between serum differential metabolites and laying performance of aged laying hens ($n = 6$). Red and blue cells represent positive and negative correlations, respectively. The significant correlations are indicated by asterisks (*$P < 0.05$, **$P < 0.01$ and ***$P < 0.001$).

of Christensenellaceae, Porphyromonadaceae, and Rikenellaceae lies in their potential to protect against cardiovascular and metabolic diseases associated with visceral adiposity (Tavella et al., 2021). Consequently, these bacterial families may serve as valuable indicators of healthy aging and, conceivably, longevity. The findings disclosed the controlled effects of ELE supplementation on the gastrointestinal microbiota of laying hens, implying a promising relationship between the intestinal microbiota and hen production.

It is widely recognized that serum metabolites can exert an impact on the metabolic processes of animals, and thereby, serve as a reliable indicator of their health status (Guasch-Ferré et al., 2016; Nicholson et al., 2012). In our investigation, we identified a total of 3 down-regulated and 12 up-regulated differential serum

metabolites that exhibited a strong correlation with both the gut microbiota and egg production performance. Numerous prospective studies have explored the significant impact of the gut microbiota on serum metabolites in both human and animal models (Dodd et al., 2017; Zhao et al., 2020). As an illustration, the biosynthesis of indole-3-propionic acid has been demonstrated to be wholly contingent upon the existence of the gut microflora and can be established through the colonization of *Clostridium sporogenes* bacterium. Additionally, the presence of gut microbes significantly augments the production of various organic acids containing phenyl groups (Wikoff et al., 2009; Dodd et al., 2017). S-adenosine-methionine, benzoic acid, 4-hydroxybenzoic acid, 2-piperidinobenzoic acid, ethyl 2-amino-8h-indendiphenol-2,1-b-thiophene-3-carboxylate, DL-methionine sulfoxide, 2-oxoglutaric
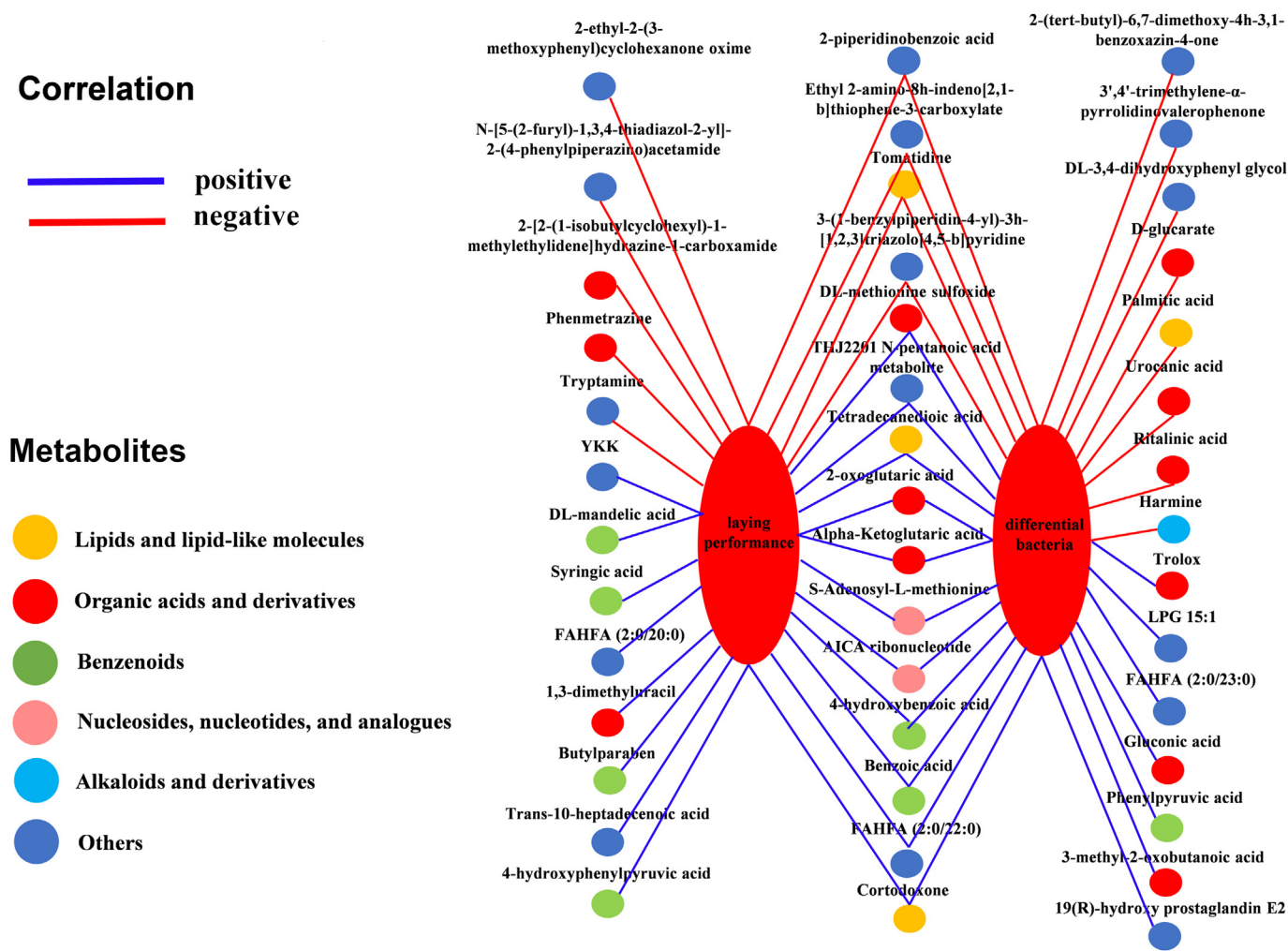
Fig. 8. Differential metabolites correlated with differential bacterial genera and laying performance by Spearman rank correlation analysis.

acid, alpha-ketoglutaric acid and 3-(1-benzylpiperidin-r-yl)-3h-[1,2,3]triazolyl[4,5-b]pyridine were shown to be favorably correlated with *Rikenellaceae_RC9_gut_group*, whilst they were negatively correlated with *Bacteroides*. Additionally, tomatidine, THJ2201N-pentanoic acid metabolite, and tetradecanedioic acid displayed a positive correlation with *Bacteroides*, while showing a negative correlation with *Rikenellaceae_RC9_gut_group*. Interestingly, these differential metabolites displayed contrasting bacterial correlations with regards to their upregulation or downregulation. It is also interesting that these metabolites are proven to improve animal performance and aid intestinal health. Relevant studies have confirmed that methionine may enhance the intestinal architecture and productivity of laying hens fed low protein diets by encouraging the growth of helpful bacteria while simultaneously preventing the growth or infection of harmful bacteria (Ma et al., 2021). S-adenosyl-L-methionine is synthesized by methionine adenosyltransferase through the utilization of adenosine triphosphate and methionine (Friedel et al., 1989; Mato et al., 1997). Benzoic acid improved the intestinal architecture and increased the microbial compositions, promoting the best possible gastrointestinal health in laying hens (Gong et al., 2021). Through changes in the intestinal microbiota, alpha-ketoglutaric acid has been shown to control intestinal energy balance, amino acid metabolism, integrity, and immunological response (He et al., 2015; Chen et al.,

2017). Recently, a plethora of studies have elucidated the close association between the gut microbiota of the host and metabolic pathways (Wang et al., 2020; Zhang et al., 2021a, 2021b). According to reports, nondigestible carbohydrates can be converted by the gut bacteria into short-chain fatty acids, which are known for their trophic, anti-inflammatory, and immunomodulatory actions that improve intestinal health (Lavelle and Sokol, 2020). Similar to this, the combination of Chinese cabbage waste and silage improves the antioxidant capacity of Hu sheep via enhancing ascorbate and aldarate metabolism via rumen Prevotellaceae UCG-004 (Li et al., 2022b). In our study, treatment with ELE was found to significantly enhance the metabolic pathways of the host, including but not limited to phenylpropane metabolism, biosynthesis of amino acids, ubiquinone and other terpenoid-quinone pathways, tryptophan and histidine metabolism, as well as ascorbate and aldarate metabolism, taurine and hypotaurine metabolism, glyoxylate and dicarboxylate metabolism, progesterone-mediated oocyte maturation, and pentose and glucuronate interconversions, fatty acid elongation, and butanoate metabolism. Taken together, our results demonstrate that dietary supplementation of ELE at 1,000 mg/kg can effectively promote intestinal health and egg production performance of aged laying hens, mediated by modulation of the abundance of gut microbiota and alterations of host metabolic pathways and serum metabolites.
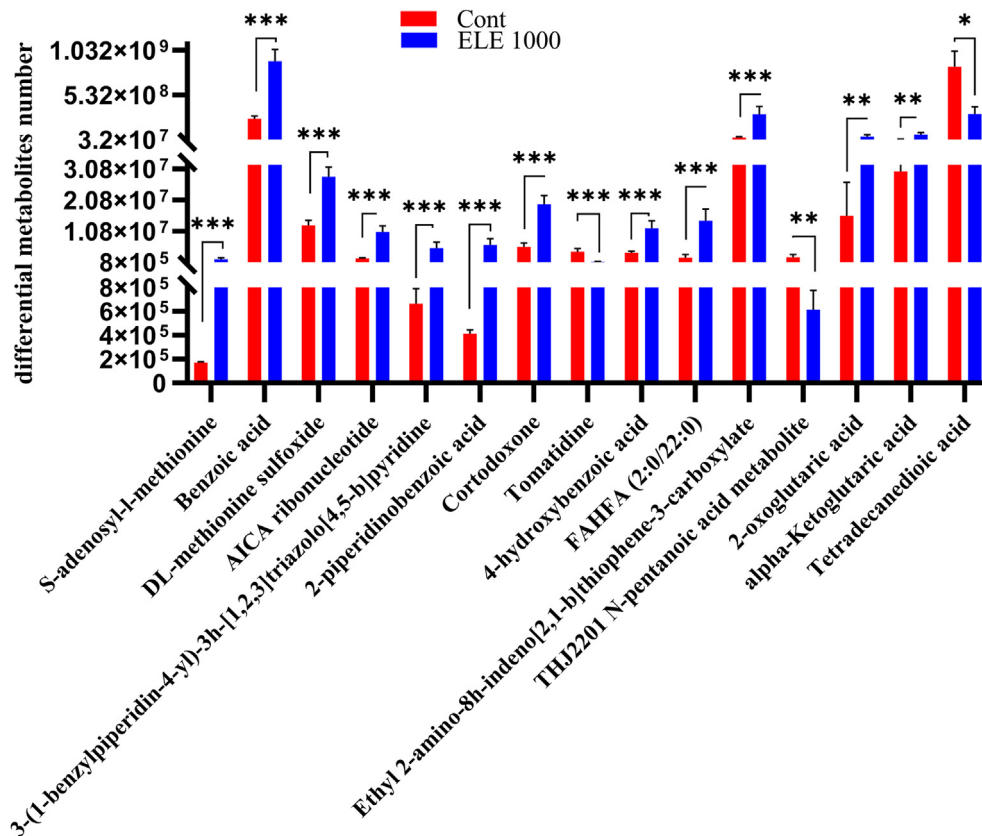
Fig. 9. *E. ulmoides* leaf extract (ELE) induced relative content change of 15 key serum differential metabolites of aged laying hens. Cont = basal diet; ELE1000 = basal diet + 1,000 mg/kg of ELE. Data are expressed as mean ± SEM ($n = 6$). *$P < 0.05$, **$P < 0.01$, ***$P < 0.001$ versus the Cont group.

5. Conclusions

The present investigation has substantiated that the inclusion of dietary ELE at a dosage of 1,000 mg/kg can ameliorate laying performance, egg quality, gut barrier function, and induce alterations in the relative abundance of intestinal flora and serum metabolites in aged laying hens. The integration of serum non-target metabolomics and 16S sequencing in conjunction with omics analysis revealed that the administration of dietary ELE at 1,000 mg/kg possesses the potential to enhance egg performance, egg quality, and gut health in aged laying hens by modulating the gut microbiome (*Bacteroides* and *Rikenellaceae_RC9_gut_group*) and subsequently influencing metabolites (e.g., DL-methionine sulfoxide, THJ2201 N-valerate metabolite, tetracarbonic acid) within the circulatory systems. Consequently, this study proposed a promising intervention wherein ELE can serve as a functional feed additive, effectively prolonging the peak laying period of aging laying hens.

Author contributions

Xiaoxiao Liang: Investigation, formal analysis, data curation, writing original draft preparation. **Yawei Fu:** Contributed to the methodology, conducted investigations, curated data, and prepared the original draft. **Hongxun Shi:** Conducted investigations and validated results. **Ruxia Wang, Kaimin Niu, Zhenya Zhai:** Reviewed and edited the manuscript. **Yulong Yin:** Conceptualized the study, reviewed and edited the manuscript, and acquired funding.

Declaration of competing interest

We declare that we have no financial and personal relationships with other people or organizations that can inappropriately influence our work, and there is no professional or other personal interest of any nature or kind in any product, service and/or company that could be construed as influencing the content of this paper.

References

Akbari P, Braber S, Gremmels H, Koelink PJ, Verheijden KA, Garssen J, et al. Deoxynivalenol: a trigger for intestinal integrity breakdown. FASEB J 2014;28(6): 2414−29.

Capaldo CT, Powell DN, Kalman D. Layered defense: how mucus and tight junctions seal the intestinal barrier. J Mol Med (Berl) 2017;95(9):927−34.

Chen S, Bin P, Ren WK, Gao W, Liu G, Yin J, et al. Alpha-ketoglutarate (AKG) lowers body weight and affects intestinal innate immunity through influencing intestinal microbiota. Oncotarget 2017;8(24):38184−92.

Dodd D, Spitzer MH, Van Treuren W, Merrill BD, Hryckowian AJ, Higginbottom SK, et al. A gut bacterial pathway metabolizes aromatic amino acids into nine circulating metabolites. Nature 2017;551(7682):648−52.

Dilawar MA, Mun HS, Rathnayake D, Yang EJ, Seo YS, Park HS, et al. Egg quality parameters, production performance and immunity of laying hens supplemented with plant extracts. Animals (Basel) 2021;11(4):975.

Dai XP, Huang Q, Zhou BT, Gong ZC, Liu ZQ, Shi SY. Preparative isolation and purification of seven main antioxidants from *Eucommia ulmoides oliv*. (du-zhong) leaves using hsccc guided by dpph-hplc experiment. Food Chem 2013;139: 563−70.

Ding HX, Cao AZ, Li HY, Zhao Y, Feng J. Effects of *Eucommia ulmoides* leaf extracts on growth performance, antioxidant capacity and intestinal function in weaned piglets. J Anim Physiol Anim Nutr (Berl) 2020;104(4):1169—77.

Friedel HA, Goa KL, Benfield P. S-adenosyl-L-methionine. A review of its pharmacological properties and therapeutic potential in liver dysfunction and affective disorders in relation to its physiological role in cell metabolism. Drugs 1989;38(3):389—416.

Guasch-Ferré M, Hruby A, Toledo E, Clish CB, Martínez-González MA, Salas-Salvadó J, et al. Metabolomics in prediabetes and diabetes: a systematic review and meta-analysis. Diabetes Care 2016;39(5):833—46.

Gong HJ, Yang ZQ, Celi P, Yan L, Ding XM, Bai SP, et al. Effect of benzoic acid on production performance, egg quality, intestinal morphology, and cecal microbial community of laying hens. Poult Sci 2021;100(1):196—205.

Hsieh CL, Yen GC. Antioxidant actions of du-zhong (*Eucommia ulmoides* Oliv.) toward oxidative damage in biomolecules. Life Sci 2000;66(15):1387—400.

Hildebrand F, Nguyen TL, Brinkman B, Yunta RG, Cauwe B, Vandenabeele P, et al. Inflammation-associated enterotypes, host genotype, cage and inter-individual effects drive gut microbiota variation in common laboratory mice. Genome Biol 2013;14(1):R4.

He LQ, Xu ZQ, Yao K, Wu GA, Yin YL, Nyachoti CM, et al. The physiological basis and nutritional function of alpha-ketoglutarate. Curr Protein Pept Sci 2015;16: 576—81.

Jing M, Munyaka PM, Tactacan GB, Rodriguez-Lecompte JC, O K, House JD. Performance, serum biochemical responses, and gene expression of intestinal folate transporters of young and older laying hens in response to dietary folic acid supplementation and challenge with Escherichia coli lipopolysaccharide. Poult Sci 2014;93(1):122—31.

Khan S, Moore RJ, Stanley D, Chousalkar KK. The gut microbiota of laying hens and its manipulation with prebiotics and probiotics to enhance gut health and food safety. Appl Environ Microbiol 2020;86(13):e00600—20.

Li HZ, Gu YF, Jin R, He QF, Zhou YM. Effects of dietary rutin supplementation on the intestinal morphology, antioxidant capacity, immunity, and microbiota of aged laying hens. Antioxidants (Basel) 2022a;11(9):1843.

Lin H, Meng LP, Sun ZZ, Sun SM, Huang XX, Lin N, et al. Yellow wine polyphenolic compound protects against doxorubicin-induced cardiotoxicity by modulating the composition and metabolic function of the gut microbiota. Circ Heart Fail 2021;14(10):e008220.

Lu YY, Fan CN, Li P, Lu YF, Chang XL, Qi KM. Short chain fatty acids prevent high-fat-diet-induced obesity in mice by regulating G protein-coupled receptors and gut microbiota. Sci Rep 2016;6:37589.

Lavelle A, Sokol H. Gut microbiota-derived metabolites as key actors in inflammatory bowel disease. Nat Rev Gastroenterol Hepatol 2020;17(4):223—37.

Li C, Chen N, Zhang XX, Shahzad K, Qi RX, Zhang ZB, et al. Mixed silage with Chinese cabbage waste enhances antioxidant ability by increasing ascorbate and aldarate metabolism through rumen Prevotellaceae UCG-004 in Hu sheep. Front Microbiol 2022b;13:978940.

Marchesi JR, Adams DH, Fava F, Hermes GD, Hirschfield GM, Hold G, et al. The gut microbiota and host health: a new clinical frontier. Gut 2016;65(2):330—9.

Martens EC, Lowe EC, Chiang H, Pudlo NA, Wu M, McNulty NP, et al. Recognition and degradation of plant cell wall polysaccharides by two human gut symbionts. PLoS Biol 2011;9(12):e1001221.

Ma ML, Geng SJ, Liu ML, Zhao LH, Zhang JY, Huang SM, et al. Effects of different methionine levels in low protein diets on production performance, reproductive system, metabolism, and gut microbiota in laying hens. Front Nutr 2021;8: 739676.

Mato JM, Alvarez L, Ortiz P, Pajares MA. S-adenosylmethionine synthesis: molecular mechanisms and clinical implications. Pharmacol Ther 1997;73(3):265—80.

Nicholson JK, Holmes E, Kinross J, Burcelin R, Gibson G, Jia W, et al. Host-gut microbiota metabolic interactions. Science 2012;336(6086):1262—7.

Peng MJ, Wang ZH, Peng S, Zhang ML, Duan YH, Li FN, et al. Dietary supplementation with the extract from *Eucommia ulmoides* leaves changed epithelial restitution and gut microbial community and composition of weanling piglets. PLoS One 2019;14(9):e0223002.

Peng MJ, Huang T, Yang QL, Peng S, Jin YX, Wang XS. Dietary supplementation *Eucommia ulmoides* extract at high content served as a feed additive in the hens industry. Poult Sci 2022;101(3):101650.

Rowland I, Gibson G, Heinken A, Scott K, Swann J, Thiele I, et al. Gut microbiota functions: metabolism of nutrients and other food components. Eur J Nutr 2018;57(1):1—24.

Rodriguez-Palacios A, Harding A, Menghini P, Himmelman C, Retuerto M, Nickerson KP, et al. The artificial sweetener Splenda promotes gut Proteobacteria, dysbiosis, and myeloperoxidase reactivity in Crohn's disease-like ileitis. Inflamm Bowel Dis 2018;24(5):1005—20.

Ryan FJ, Ahern AM, Fitzgerald RS, Laserna-Mendieta EJ, Power EM, Clooney AG, et al. Colonic microbiota is associated with inflammation and host epigenomic alterations in inflammatory bowel disease. Nat Commun 2020;11(1):1512.

Shi SY, Guo KK, Tong RN, Liu YG, Tong CY, Peng MJ. Online extraction-hplc-frap system for direct identification of antioxidants from solid du-zhong brick tea. Food Chem 2019;288:215—20.

Sun WT, He M, Xu XY, Li XQ, Pan WQ, Leng XJ. Comparison study of three compounds in *Eucommia ulmoides* on growth, flesh quality of grass carp (Ctenopharyngodon idella). Aquacult Nutr 2019:906—16.

Sun B, Hou L, Yang Y. The development of the gut microbiota and short-chain fatty acids of layer chickens in different growth periods. Front Vet Sci 2021;8: 666535.

Tavella T, Rampelli S, Guidarelli G, Bazzocchi A, Gasperini C, Pujos-Guillot E, et al. Elevated gut microbiome abundance of Christensenellaceae, Porphyromonadaceae and Rikenellaceae is associated with reduced visceral adipose tissue and healthier metabolic profile in Italian elderly. Gut Microbes 2021;13(1):1—19.

Wikoff WR, Anfora AT, Liu J, Schultz PG, Lesley SA, Peters EC, et al. Metabolomics analysis reveals large effects of gut microflora on mammalian blood metabolites. Proc Natl Acad Sci U S A 2009;106(10):3698—703.

Wang DT, Guo SP, He HX, Gong L, Cui HZ. Gut microbiome and serum metabolome analyses identify unsaturated fatty acids and butanoate metabolism induced by gut microbiota in patients with chronic spontaneous urticaria. Front Cell Infect Microbiol 2020;10:24.

Xing YF, He D, Wang Y, Zeng W, Zhang C, Lu Y, et al. Chemical constituents, biological functions and pharmacological effects for comprehensive utilization of *Eucommia ulmoides* Oliver. Food Sci Hum Well 2019;8(20):177—88.

Xiong BH. Chinese feed composition and nutritional value table (32th edition, 2021) Chinese feed database. Chin J Anim Husb 2021;23(1):97.

Yan JH, Hu RZ, Li BZ, Tan JJ, Wang Y, Tang ZY, et al. Effect of *Eucommia ulmoides* leaf extract on growth performance, carcass traits, parameters of oxidative stress, and lipid metabolism in broiler chickens. Front Vet Sci 2022;9:945981.

Zhang Q, Zhang KY, Wang JP, Bai SP, Zeng QF, Peng HW, et al. Effects of coated sodium butyrate on performance, egg quality, nutrient digestibility, and intestinal health of laying hens. Poult Sci 2022a;101(9):102020.

Zhao JS, Deng W, Liu HW. Effects of chlorogenic acid-enriched extract from *Eucommia ulmoides* leaf on performance, meat quality, oxidative stability, and fatty acid profile of meat in heat-stressed broilers. Poult Sci 2019;98(7): 3040—9.

Zhai ZY, Niu KM, Liu YC, Lin C, Wu X. The gut microbiota-bile acids-TGR5 axis mediates *Eucommia ulmoides* leaf extract alleviation of injury to colonic epithelium integrity. Front Microbiol 2021;12:727681.

Zhang FL, Hao Q, Zhang QS, Lv HY, Yang YL, Chao-Ran, et al. Influences of dietary *Eucommia ulmoides* leaf extract on the hepatic lipid metabolism, inflammation response, intestinal antioxidant capacity, intestinal microbiota, and disease resistance of the channel catfish (Ictalurus punctatus). Fish Shellfish Immunol 2022b;123:75—84.

Zhao X, Wang YJ, Nie ZY, Han LF, Zhong XQ, Yan XH, et al. *Eucommia ulmoides* leaf extract alters gut microbiota composition, enhances short-chain fatty acids production, and ameliorates osteoporosis in the senescence-accelerated mouse P6 (SAMP6) model. Food Sci Nutr 2020;8(9):4897—906.

Zhang X, Coker OO, Chu ES, Fu K, Lau HCH, Wang YX, et al. Dietary cholesterol drives fatty liver-associated liver cancer by modulating gut microbiota and metabolites. Gut 2021a;70(4):761—74.

Zhang J, Feng D, Law HK, Wu Y, Zhu GH, Huang WY, et al. Integrative analysis of gut microbiota and fecal metabolites in rats after prednisone treatment. Microbiol Spectr 2021b;9(3):e0065021.

Zhang LY. Feed analysis and feed quality testing technology. 3rd ed. Beijing: China Agricultural Press; 2007.